LAND SURFACE TEMPERATURE RETRIEVAL BY RADIATIVE TRANSFER EQUATION AND SINGLE CHANNEL ALGORITHMS USING LANDSAT-8 SATELLITE DATA

Abhishek Danodia*, Bhaskar R. Nikam, Suresh Kumar, N.R. Patel
Indian Institute of Remote Sensing- ISRO, 4- Kalidas road, Dehradun-248001
*Email: abhidanodia@iirs.gov.in

KEYWORDS: Land surface temperature, Radiative Transfer Equation, Single Channel algorithm, Landsat-8, Land surface emissivity.

ABSTRACT: Land surface temperature (LST) is the key parameter which in land surface processes, energy balance, crop evapotranspiration, water allocation and planning from small to larger extant on globe. Now a day, LST retrieval algorithms become a research interest globally using various satellite data at different spatial resolution. In the present study, the main aim is to retrieve land surface emissivity and temperature over the parts of North India using Radiative Transfer Equation (RTE) based method and Single Channel (SC) method for the *Rabi* season using Landsat-8 thermal infra-red sensor (TIR) data. The main task in LST retrieval is removing the atmospheric attenuation effects and calculation of land surface emissivity (LSE) with vegetation variability which was incorporated in LSE. So, NDVI was estimated as proxy of vegetation which is varied with crop cover. Upwelling and downwelling path radiance with atmospheric transmittance are estimated from MODTRAN model for TIRS. These radiances were incorporated in estimation of complex process of LSE. RTE and SC algorithms assimilate the thermal radiance measured at sensor level, accompany with emissivity. Mean LST varied from 302.3°K to 276.5°K and 307.7°K to 282.0°K derived from RTE method and SC method, respectively for all kind of land covers available in the study area. NDVI values were compared with respective LST values for understanding the LST association with NDVI. A strong negative correlation was observed between NDVI and LST (R^2 = 0.80 for RTE method and R^2 = 0.84 for SC method), especially in vegetated areas. However, calculation of emissivity due to change in vegetation with spatial scale is complex and matter of future research studies.

1. INTRODUCTION

Land surface temperature (LST) is the key parameters for better understanding the physics behind the geo- biophysical phenomena of the earth surface (Jiménez-Muñoz et al., 2014). In recent years, the applications of thermal data are significantly increase in all kind of earth observations based research applications like agricultural water management, water resources management, estimation of crop evapotranspiration, energy balance study, climate change, hydrological cycle, vegetation monitoring, urban climate and environmental studies, etc. (Kerr et al., 2000; Sobrino et al., 2004; Anderson et al., 2008; Jiménez-Muñoz et al., 2014). LST varies rapidly with space and time due to heterogeneity of surface parameters like soil, water, vegetation and because of this ground measurements are not reliable over wide areas. Remote sensing can assist us to measure LST for entire globe with a fine spatial and temporal resolution rather than point observations (Liu et al., 2006; Neteler, 2010; Li et al., 2013). Remote sensing satellite-based Thermal Infra-Red (TIR) data is measured by the on-board satellite radiometer in term of radiances in TIR spectral region. TIR data is further used for LST retrieval using various radiation and emissivity equation-based methods. The accuracy of LST retrieval method is the area of research because it is not only dependent on surface/ terrain parameters (temperature and emissivity) but also on the atmosphere and its characteristics (Prata et al., 1995).

The Landsat projects make available the opportunity for LST retrieval using thermal band since Landsat 4 and 5, had the Thematic Mapper (TM), following by the Enhanced Thematic Mapper Plus (ETM+) of Landsat 7. The last launch of Landsat 8 satellite ensures more numbers of spectral bands in this remote sensing data as compare to all previous Landsat missions such as TM and ETM+. Landsat 8 has two sensors; the Operational Land Imager (OLI) and the Thermal Infrared (TIR). OLI collects data in eight bands located in visible and near infrared region and short-wave infrared regions of the electro-magnetic spectrum at a 30 meter spatial resolution add-on an additional panchromatic band at 15 meter spatial resolution. TIR sensor has two bands located in the atmospheric window between 10 and 12 µm, acquire the TIR radiance at 100 meter spatial resolution, but are resampled to 30 m in delivered data product.

The LST can be estimated by several methodologies or algorithms like LST retrieval with known LSE (single channel method, multi-channel method, and multi-angle method), LST retrieval with unknown LSE (Simulation techniques and

stepwise LSE retrieval method, using different methods to deal with the emissivity and atmospheric effects (Qin et al., 2001; Jiménez-Muñoz and Sobrino, 2003; Li et al., 2013). For the RTE-based method, the atmospheric profile was extracted from the NCEP (National Centre for Environmental Prediction) data set and used to simulate atmospheric transmittance, upwelling and downwelling from the MODTRAN (MODerate resolution atmospheric TRANsmission) model (Yu et al., 2014). For the SC method, a novel algorithm from Sobrino (2004) was used. The land surface emissivity (LSE) was derived from a NDVI (Normalized Difference Vegetation Index) threshold method (Sobrino and Raissouni, 2000). The comparison has been made using two LST retrieval methods over a crop prominent terrain of North India. The aims of this study were: (1) to analyzing these two methods for LST estimation from the Landsat 8 satellite data and (2) to derive a relationship between LST and NDVI for the study area.

2. STUDY AREA AND DATA USED

2.1. Study area

The study has been carried out in parts of Western Uttar Pradesh, India. The study area comprises Meerut, Muzaffarnagar, Baghpat districts of Uttar Pradesh (Fig. 1). Agro-horticulture and agro-forestry are emerging enterprises of farming system in this region. The dominant cropping system is sugarcane- wheat followed by rice- wheat cropping system in this area. Sugarcane and wheat are the predominant commercial crops cultivated in this irrigated regions. The soil of this area is alluvium, coarse to medium in texture and moderately alkaline, appears dark gray indicating high organic matter content (Danodia et al., 2017).

2.2. Data used

One cloud-free Landsat-8 image of the study area (acquired on 10th December 2014) was downloaded from the USGS website (http://glovis.usgs.gov/) and analyzed in this study, covering *Rabi* crop season of 2014-15.

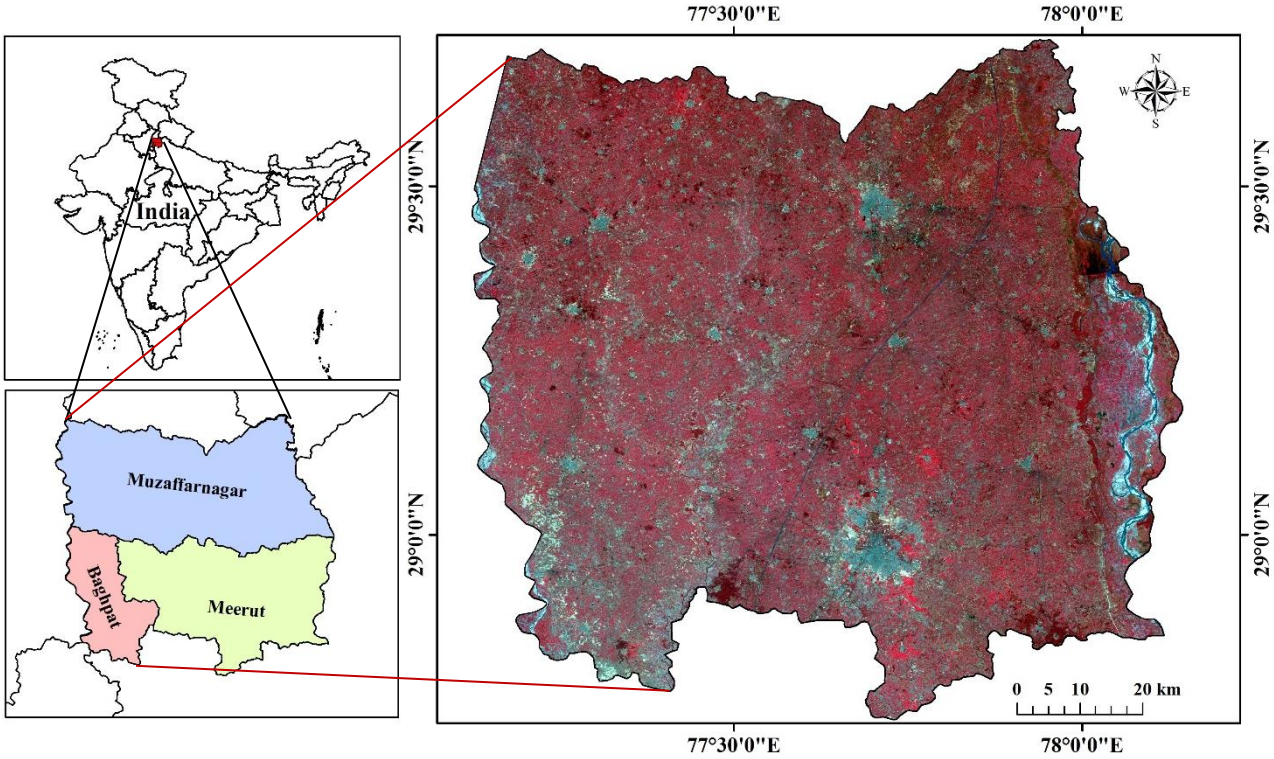

Figure 1: Location map of study area with Standard False Color Composite generated from Landsat 8 OLI data (acquired on 10th December 2014).

In the present study the LULC (Land Use Land Cover) map (Fig. 2), derived using multi-spectral data from Resourcsat-1 AWiFS sensor, which is available at Bhuvan ISRO's Geo-portal (www.bhuvan.nrsc.gov.in), was used for understanding of LST spatial variation with various land cover in the study area.

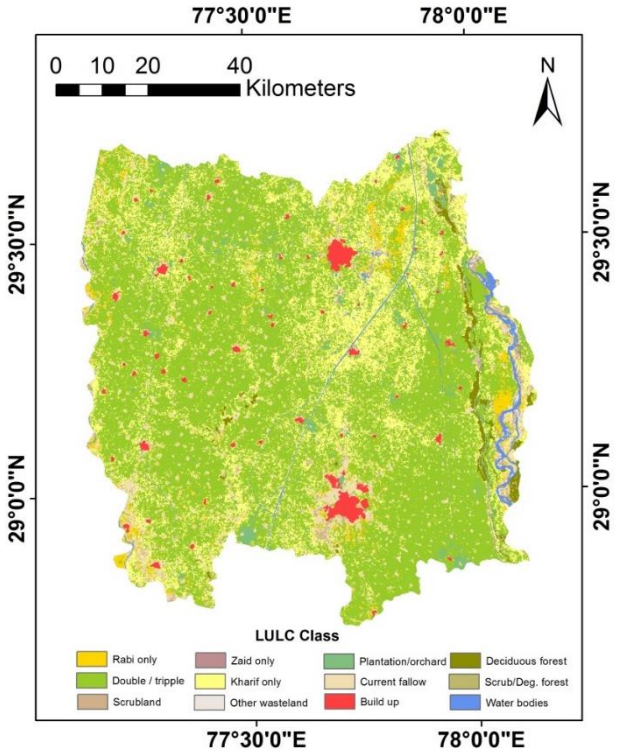

Figure 2: LULC map of study area (source: *bhuvan*).

3. METHODOLOGY

3.1. NDVI estimation

NDVI image shows the vegetation extent of the area by analysing near infrraed and red spectral band data. NDVI is the index of photosynthetic activity in plant and it is the most commonly used vegetation spectral indices for crop growth monitoring. NDVI always ranges from -1 to +1 but there are not any distinct boundary for each type of land cover. In present case NDVI is calculated by using band 4 (red band) and band 5 (near infrared band) data of L8 OLI sensors for assessment of live green vegetation or not (Eq. 1). NDVI can be expressed as (Tucker, 1979):

$$NDVI = \frac{NIR-R}{NIR+R} \qquad (1)$$

where, NIR is the reflectance of near infrared band and R is the reflectance of red band.

The NDVI image was further used in NDVI based emissivity assessment and establishing NDVI-LST relationship to understanding about LST trend of various land covers as NDVI varied.

3.2. Estimation of Land Surface Emissivity (LSE)

LSE is necessary parameter for LST inversion. The emissivity of surface varies with vegetation, soil moisture, roughness and viewing angles. Three major methods are recommended in literature for LSE estimation for LST inversion: i) classification- based emissivity method (CBEM), ii) NDVI- based emissivity method (NBEM) and iii) day/ night temperature- independent spectral indices based method (TISI) (Yu et al., 2014). In this study, NBEM was implemented for LSE estimation using NDVI derived from Landsat 8 OLI data. NDVI was classified in three classes:

(a.) bare soil: NDVI < 0.2, (b.) mixture of bare soil and vegetation: 0.2 ≤ NDVI ≤ 0.5 and (C.) fully vegetated: NDVI > 0.5. LSE for each of these classes is estimated using the following equation (Sobrino et al., 2004; Yu et al., 2014: Nikam et al., 2016):

$$\varepsilon_i = \begin{cases} a_i \rho_{red} + b_i & NDVI < 0.2 \\ \varepsilon_{v,i} P_v + \varepsilon_{s,i}(1 - P_v) + C_i & 0.2 \leq NDVI \leq 0.5 \\ \varepsilon_{v,i} + C_i & NDVI > 0.5 \end{cases} \quad (2)$$

Where, ρ_{red} is the reflectance of red band, P_v is the fraction of vegetation, ε_s and ε_v is the emissivity of soil and vegetation and a_i, b_i, C_i are the essential coefficients which are discussed in Yu et al. (2014).

3.3. LST retrieval method

In the present study the LST of the study area has been retrieved using two algorithms namely RTE (Radiative Transfer Equation) and SC (Single Channel). Brief description of each of this method is given in subsequent sub-sections.

3.3.1. Radiation Transfer Equation method

In this method, TIR band was used for LST estimation from Landsat 8 imagery as the following equation (Sobrino et al., 2004; Yu et al., 2014):

$$L_{sensor,\lambda} = \left[\varepsilon_\lambda B_\lambda(T_s) + (1 - \varepsilon_\lambda) L^{\downarrow}_{atm,\lambda}\right]\tau_\lambda + L^{\uparrow}_{atm,\lambda} \quad (3)$$

where, L_{sensor} is the Top of Atmospheric (TOA) radiance, ε is the land surface emissivity, $B(T_s)$ is the blackbody radiance given by the Planck's law and T_s is the LST, $L^{\downarrow}_{atm}$ is the downwelling atmospheric radiance, τ is the total atmospheric transmissivity between the surface and the sensor and $L^{\uparrow}_{atm}$ is the upwelling atmospheric radiance. Therefore, from Eq. (3) it is possible to find T_s by inversion of the Planck's law as:

$$T_s = \frac{C_1}{\lambda_i ln\left(\frac{C_2}{\lambda_i^5\left(L_{sensor,\lambda} - L^{\uparrow}_{atm} - \tau_\lambda(1-\varepsilon_\lambda)L^{\downarrow}_{atm}\right)/\tau_\lambda\varepsilon_\lambda} + 1\right)} \quad (4)$$

where, T_s is the land surface temperature, λ_i is the effective band wavelength for band i, C_1 is 14387.7 μm.°K and C_2 is $1.19104*10^8$ W.μm^4.m^{-2}.sr^{-1}.

With the thermal radiance data measured by TIR sensor, accompany with atmospheric parameters, the LST can be retrieved according to Eq. (4). The atmospheric parameters τ, $L^{\downarrow}_{atm}$ and $L^{\uparrow}_{atm}$ was estimated from the NCEP datasets and simulated using MODTRAN model. As for the LSE, it is discussed in the section 3.2.

3.3.2. The Jiménez-Muñoz and Sobrino's Single- Channel method

Jiménez-Muñoz and Sobrino (2003) have developed a single- channel method for retrieval LST from thermal band, in which LST is depicted in following equation:

$$T_s = \gamma[\varepsilon^{-1}(\psi_1 L_{sensor} + \psi_2) + \psi_3] + \delta \quad (5)$$

With

$$\gamma = \left\{\frac{C_2 L_{sensor}}{T^2_{sensor}}\left[\frac{\lambda^4}{C_1} L_{sensor} + \lambda^{-1}\right]\right\}^{-1} \quad (6)$$

$$\delta = -\gamma L_{sensor} + T_{sensor} \quad (7)$$

where, T_{sensor} is the at- sensor brightness temperature in °K. The atmospheric functions ψ_1, ψ_2 and ψ_3 can be acquired as a function of the total atmospheric water vapor content (w). Those parameters can be parameterized as a third degree regression with the thermal band's wavelength as well discussed in Yu et al. (2014). Those atmospheric functions ψ_1, ψ_2 and ψ_3 are unit-less and derived from water vapor content available in atmospheric water column using MODTRAN model.

4. RESULTS AND DISCUSSIONS

Figure 3 depicted the NDVI image generated using Landsat 8 OLI data of the study area acquired on 10th December 2014. Here, the maximum and the minimum NDVI was 0.79 and -0.59, respectively. Higher value of NDVI shows the more dense vegetation (forest/orchard) while lower value shows the water bodies. Mean NDVI of crop, fallow, orchad, forest, wateland and urban were 0.39, 0.08, 0.43, 0.43, 0.1 and 0.09, respectively.

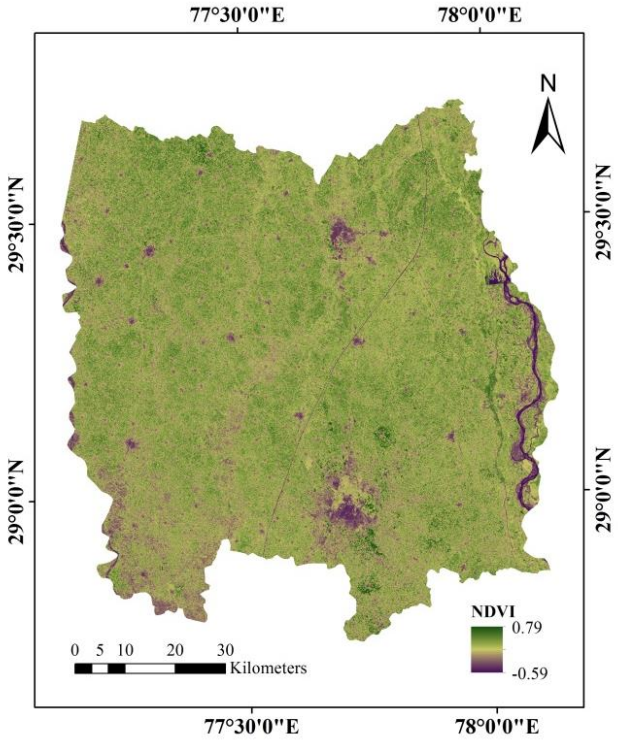

Figure 3: NDVI map generated from Landsat 8 OLI data acquired on 10th December 2014.

LST image defines the skin temperature of surface which can be formulated using various techniques, mentioned above. In this study, RTE and SC algorithm was used for LST retrieval and a relationship was formulated between LST and NDVI for both of the methods for Landsat 8 imagery acquired on 10th December, 2014 (Fig. 4). Mean LST varied from 302.3°K to 276.5°K in RTE derived results whereas it varies from 307.7°K to 282.0°K is SC derived products for all kind of LULC classes in the study area. The highest mean LST was analyzed for fallow land as 287.4°K and 293.1°K while the lowest mean LST was analyzed for forest and orchard land as 285.7°K and 290.2°K derived from RTE and SC method, respectively. Agriculture land had 286.8°K and 291.4°K LST resulting from RTE and SC algorithm.

Healthy vegetation represents vigor and greenness which can be directly correlated with NDVI as well as crop conditioning. High values of NDVI are depicted the crop, orchard and forest as a result of high levels of green biomass while low values of NDVI represents the bare soil and urban area. The scatter plot was generated between NDVI and LST derived from both methods (Fig. 5). Here, LST had a significant negative correlation with NDVI (R^2 = 0.80 for RTE method and R^2 = 0.84 for SC method) for agriculture land class. It means an area which has more vegetation are having low temperature because available energy are portioning more towards evapotranspiration process, so that LST will be lesser as compare low vegetation area. Scanty vegetation has also higher LST due to low NDVI value. The strong negative correlation between NDVI and LST established in the present study is in agreement with previous studies of Nemani and Running (1989), Sun and Kafatos (2007) and Yue et al. (2007).

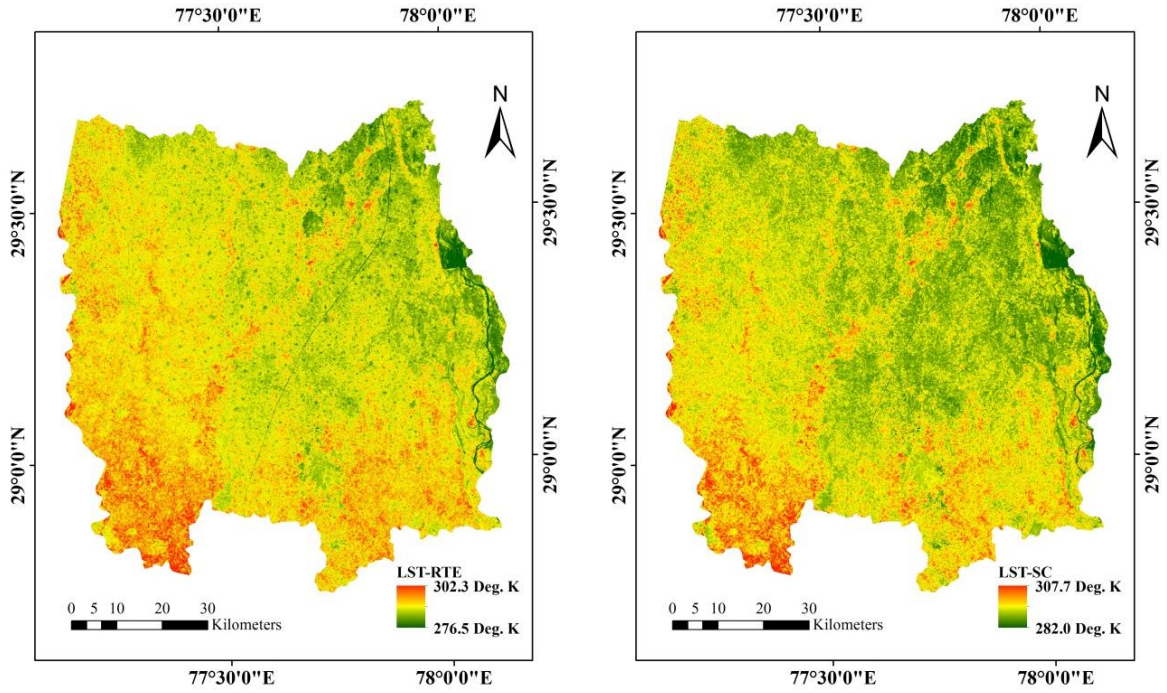

Figure 4: LST images derive from RTE and SC method from Landsat 8 TIR data.

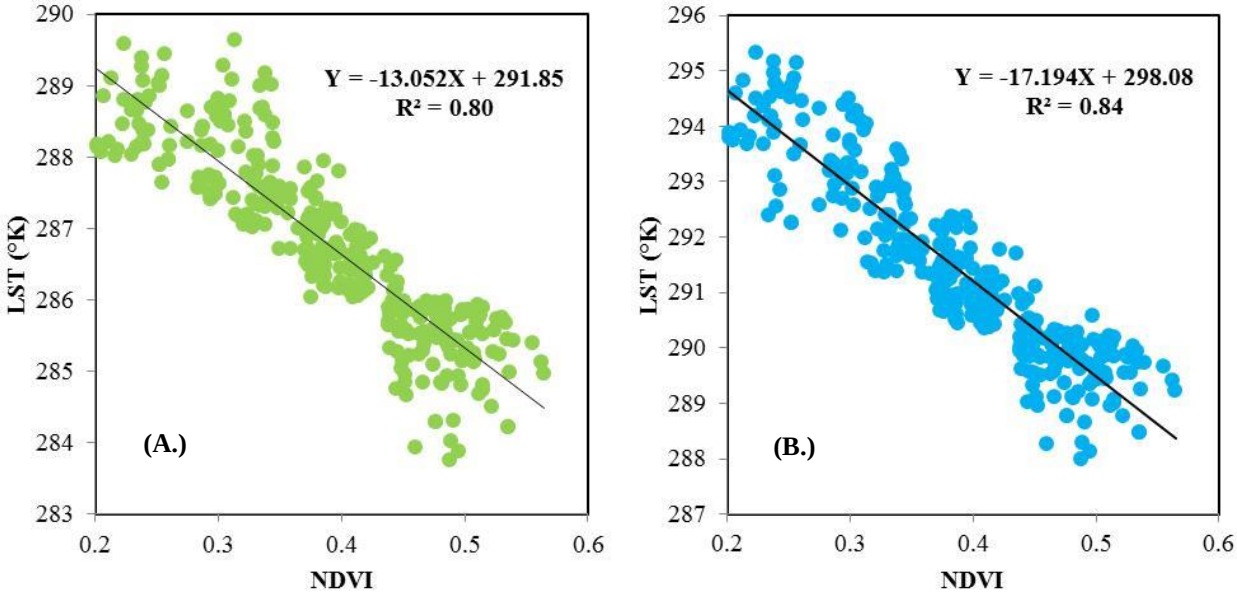

Figure 5: Scatter plot between LST and NDVI for (A.) RTE, (B.) SC.

5. CONCLUSIONS

The present study was discussed about two techniques: RTE and SC algorithm of LST retrieval. Mean LST varied from 302.3°K to 276.5°K and 307.7°K to 282.0°K, derived from RTE method and derived from SC method, respectively for the study area. LST had a significant negative correlation with NDVI (R^2 = 0.80 for RTE method and R^2 = 0.84 for SC method) for agriculture land class. Hence, SC algorithm derived LST was more associated with NDVI as compare to RTE method. In LSE estimation, emissivity is crucial parameter which is varied with different land covers and always a domain of research for better estimation of emissivity for all kind of land feathers.

6. REFERENCES

Anderson, M. C., Norman, J. M., Kustas, W. P., Houborg, R., Starks, P. J., Agam, N., 2008. A thermal-based remote sensing technique for routine mapping of land-surface carbon, water and energy fluxes from field to regional scales. Remote Sensing of Environment, 112, pp. 4227–4241.

Danodia, A., Patel, N. R., Chol, C. W., Nikam, B. R., Sehgal, V. K., 2017. Application of S-SEBI model for crop evapotranspiration using Landsat-8 data over parts of North India. Geocarto International. (DOI: 10.1080/10106049.2017.1374473)

Jiménez-Muñoz, J. C., Sobrino, J. A., 2003. A generalized single-channel method for retrieving land surface temperature from remote sensing data. Journal of Geophysical Research, 108 (doi: 10.1029/ 2003JD003480).

Jiménez-Muñoz, J. C., Sobrino, J. A., Skokovi´c, D., Mattar, C., Cristóbal, J., 2014. Land Surface Temperature Retrieval Methods from Landsat-8 Thermal Infrared Sensor Data. IEEE Geoscience and Remote Sensing Letters, 11 (10), pp. 1840-1843.

Kerr, Y. H., Lagouarde, J. P., Nerry, F., & Ottlé, C., 2000. Land surface temperature retrieval techniques and applications. In D. A. Quattrochi, & J. C. Luvall (Eds.), Thermal remote sensing in land surface processes, Boca Raton, Fla.: CRC Press, pp. 33–109.

Li, Z., Tang, B., Wu, H., Ren, H., Yan, G., Wan, Z., Trigo, I. F., Sobrino, J. A., 2013. Satellite-derived land surface temperature: Current status and perspectives. Remote Sensing of Environment, 131, pp. 14-37.

Liu, Y., Hiyama, T., & Yamaguchi, Y., 2006. Scaling of land surface temperature using satellite data: A case examination on ASTER and MODIS products over a heterogeneous terrain area. Remote Sensing of Environment, 105, pp. 115–128.

Nemani, R. R., Running, S. W., 1989. Estimation of regional surface resistance to evapotranspiration from NDVI and thermal- IR AVHRR Data. Journal of Applied Meteorology, 28, pp. 276–284.

Neteler, M., 2010. Estimating daily land surface temperatures in mountainous environments by reconstructed MODIS LST Data. Remote Sensing, 2, pp. 333–351.

Nikam, B. R., Ibragimov, F., Chouksey, A., Garg, V., Aggarwal, S. P., 2016. Retrieval of land surface temperature from Landsat 8 TIRS for the command area of Mula irrigation project. Environmental Earth Sciences, 75, pp. 1-17.

Pirottia, F., Parraga, M. A., Stuaro, E., Dubbini, M., Masiero, A., Ramanzin, M., 2014. NDVI from Landsat 8 vegetation indices to study movement dynamics of Capra ibex in mountain areas. In: ISPRS Technical Commission VII Symposium; XL-7, pp. 147-153.

Prata, A. J., Caselles, V., Coll, C., Sobrino, J. A., & Ottlé, C., 1995. Thermal remote sensing of land surface temperature from satellites: Current status and future prospects. Remote Sensing Reviews, 12, pp. 175–224.

Sobrino, J. A., Jiménez-Muñoz, J. C., Paolini, L., 2004. Land surface temperature retrieval from LANDSAT TM 5. Remote Sensing of Environment, 90, pp. 434-440.

Sobrino, J. A., Raissouni, N., 2000. Toward remote sensing methods for land cover dynamic monitoring: application to Morocco. International Journal of Remote Sensing, 21, pp. 353–366.

Sun, D., Kafatos, M., 2007. Note on the NDVI-LST relationship and the use of temperature-related drought indices over North America. GEOPHYSICAL RESEARCH LETTERES, 34, L24406, pp. 1-4.

Tucker, C. J., 1979. Red and photographic infrared linear combinations for monitoring vegetation. Remote Sensing Environment, 8, pp. 127-150.

Yu, X., Guo, X., Wu, Z., 2014. Land Surface Temperature Retrieval from Landsat 8 TIRS- Comparison between Radiative Transfer Equation-Based Method, Split Window Algorithm and Single Channel Method. Remote sensing, 6, pp. 9829-9852.

Yue, W., Xu, J., Tan, W., Xu, L., 2007. The relationship between land surface temperature and NDVI with remote sensing: application to Shanghai Landsat 7 ETM+ data, 28 (15), pp. 3205-3226.